Proximate Bases of Silver Color in Anhinga (*Anhinga anhinga*) Feathers

Matthew D. Shawkey,* Rafael Maia, and Liliana D'Alba

Integrated Bioscience Program, Department of Biology, The University of Akron, Akron, Ohio 44325

ABSTRACT Colors of living organisms are produced by selective light absorption from pigments and/or by light scattering from highly ordered nanostructures (i.e., structural color). While the physical bases of metallic colors of arthropods and fish are fairly well-known, those of birds are not. Here we examine structurally based silver color and its production in feathers of the waterbird species *Anhinga*. This achromatic color is distinguished from grey by high specular reflectance, from white by low diffuse reflectance, and from both by high gloss. Light and electron microscopy revealed three modifications of feathers likely leading to silver color. First, proximal barbules were highly elongated and contained glossy black color at their base and white color at their pennulum. Second, this glossy black portion contained a single outer layer of keratin weakly bounded by melanosomes. Finally, the white portion contained a disordered amorphous matrix of keratin and air. Optical analyzes suggest that these structures produce, respectively, glossy black color through thin-film interference and white color through incoherent light scattering. Silver color likely results from the combined reflectance of these adjacent structures. This represents a distinct mechanism for attaining silver colors that may have been partially derived through selection for display, thermoregulation or decreased hydrophobicity. J. Morphol. 000:000–000, 2011.

KEY WORDS: structural color; feathers; biophotonics

INTRODUCTION

Coloration of living organisms is produced by differential absorption of light by pigments (e.g., carotenoids, melanins) and/or by scattering of light from biological nanostructures (Fox, 1976; Hill and McGraw, 2006). These nanostructures have diverse morphologies ranging from laminar arrays to three-dimensional matrices and produce a startling array of colors from deep ultraviolet to red (Prum, 2006; Shawkey et al., 2009). In birds, noniridescent structural feather colors are typically created by matrices of keratin and air forming a single medullary layer within feather barbs (termed a spongy layer (Shawkey et al., 2006a) or nanofiber array (D'Alba et al., 2011)), whereas iridescent colors are typically created by stacks of melanin granules within a keratin substrate in feather barbules (Prum, 2006). One of the simplest iridescent nanostructures is a single one-dimensional organized layer of melanin granules or air surrounded by a thin (60–650 nm) keratin cortex that produces color by thin-film interference. Recently, thin film-like structures with weakly organized melanosomes beneath a thin keratin cortex have been shown to produce glossy black color (Maia et al., 2010).

While the most well-studied structural colors are chromatic, achromatic white structural colors in rock ptarmigan (*Lagopus muta*) feathers (Dyck, 1979) and *Cyphochilus* beetle cuticle (Vukusic et al., 2007) and metallic silver structural colors in the cuticles of beetles like *Chrysina chrysagyrea* (Seago et al., 2008) and the scales of fish (Levy-Lior et al., 2010) have been described. The former colors are produced by amorphous matrices of keratin/chitin and air, whereas the latter are produced by multilayer thin films of chitin/guanine that act as broadband reflectors. The presence of silver colors in feathers of several bird species was first noted almost a century ago (Chandler, 1916) and more recently by Galván et al. (2009). While these silver feather colors look similar to those in fish and beetles, they do not show an accentuated metallic appearance, suggesting that they may have fundamentally different nanostructures. Both Chandler (1916) and Galván et al. (2009) noted that silver feathers displayed modified flattened barbules overlapping an otherwise black feather but did not describe their nanostructure. Understanding the nanostructures involved in producing this unique color is required to improve our understanding of the function, mechanisms of production, and evolution of silver feathers, as well as potentially provide inspiration for novel biomimetic optical nanostructures.

Contract grant sponsor: U. Akron startup funds and AFOSR; Contract grant number: FA9550-09-1-0159.

*Correspondence to: Matthew D. Shawkey; Integrated Bioscience Program, Department of Biology, The University of Akron, Akron, OH 44325. E-mail: shawkey@uakron.edu

Received 4 February 2011; Revised 3 May 2011;
Accepted 21 May 2011

Published online 00 Month 2011 in
Wiley Online Library (www.interscience.wiley.com)
DOI: 10.1002/jmor.10993

Fig. 1. Picture of an Anhinga (*Anhinga anhinga*) illustrating spread-wing posture and silver wing covert and scapular feathers. Photo by Erika Ritter, permission granted to reproduce.

Thus, we examined bright silver color in Anhinga (Aves, Anhingidae: *Anhinga anhinga*) feathers. This color is found in the wing coverts and scapular feathers and is particularly conspicuous when it adopts its characteristic "wing spread" posture (Fig. 1; Frederick and Siegel-Causey, 2000). These silver feathers are distinguished to the human eye by a "shine" or gloss that is characteristic of iridescent and glossy black feathers (Maia et al., 2010). We first used multiple techniques of UV–vis spectrometry to quantify this color and compare it to that of typical white and grey feathers. Then, we identified the proximate bases of the color using a refractive index-matching experiment, light and electron microscopy, and optical modeling.

MATERIALS AND METHODS

We pulled black and silver Anhinga scapular feathers from a study specimen in the Ornithological Collection at the University of Akron. No information on specimen age or sex was available, so we cannot address the issues of dichromatism or possible degradation with aging (e.g., Toomey et al., 2010). However, the feathers appeared bright and in good condition. To compare properties between the colors of grey and silver feathers, and

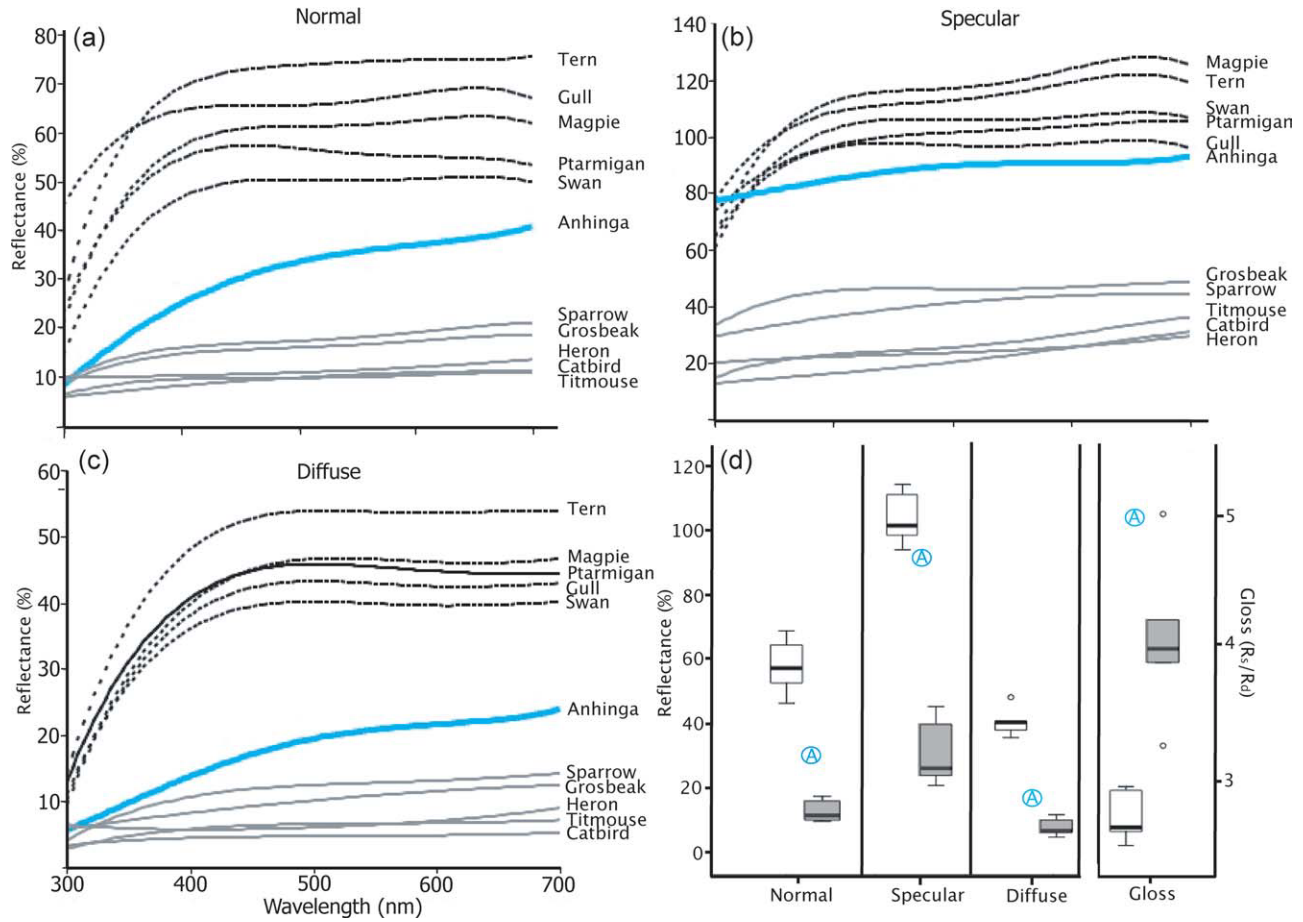

Figure 2.

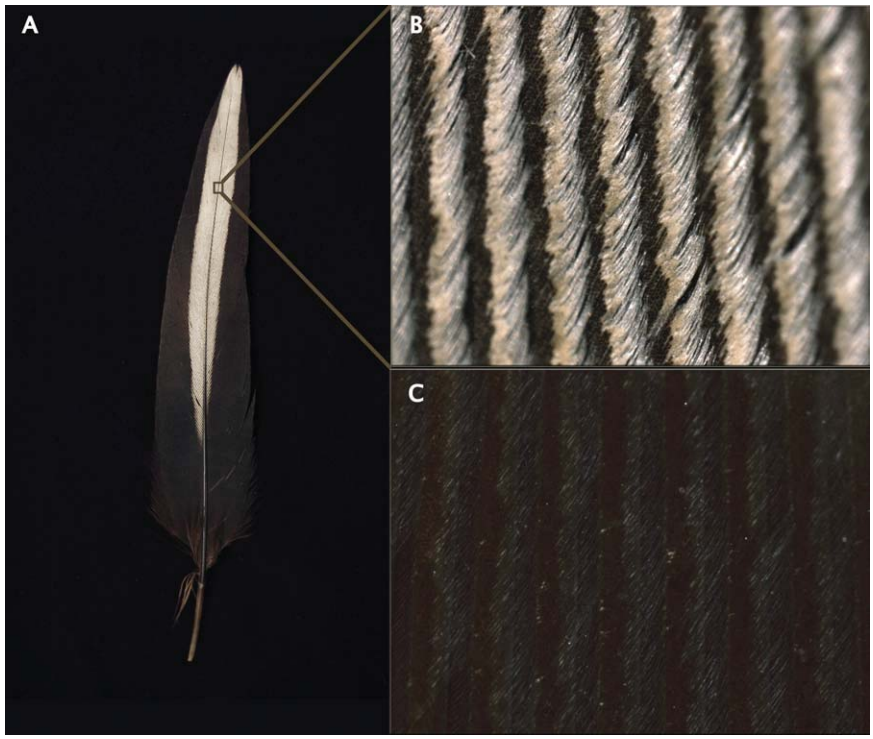

Fig. 3. Experimental demonstration of the structural basis of silver color in Anhinga feathers. A: Anhinga scapular feather. B: Closeup of the silver portion of an Anhinga feather showing distinct white and black portions. C: Closeup of this same silver portion after application of an oil with the same refractive index as keratin. The loss of the white color, and hence the silver color, indicates that it is caused by light scattering at interfaces of keratin and air.

because silver barbules had large white sections (see Fig. 3), we pulled grey and white contour feathers from study specimens of 10 other species (five of each color type; see Table 1). Because no live vertebrate animals were used in this study, Institutional Animal Care and Use Committee protocols were not needed.

Spectrometry

Light can be reflected from any surface or structure either specularly (at the same angle that it strikes the material), or diffusely (scattered equally at most other angles; Nassau, 1983). Specular and diffuse reflectances are sometimes referred to as "mirror-like" and "cloud-like" reflectance, respectively. Gloss can be measured as the ratio of specular ("mirror-like") to diffuse ("cloud-like") reflectance, with high ratios indicating high gloss (Nickerson, 1957; Rasmussen and Dyck, 2000). We hypothesized that silver Anhinga feathers had higher gloss than grey feathers. To quantify gloss and test this hypothesis, we measured diffuse and specular reflectance from these feathers using UV–vis spectrometry. For all reflectance measurements, we taped either single (Anhinga) or directly overlaid stacks of three (other species) feathers to black velvet. While barbules of scapular Anhinga feathers interlock and prevent the reflectance of light from the surface below the feather, those from contour feathers of the other species do not. Thus, overlapping contour feathers was necessary to prevent measurement of the surface below them. Reflectance was measured from these stacks using an Avantes AvaSpec-2048 spectrometer and AvaLight-XE pulsed xenon light source, relative to a WS-2 white reflectance standard (Avantes, Boulder, CO).

To quantify specular reflectance, we took point source reflectance measurements using two separate probes both placed at 75° from the normal plane (herafter, "specular measurements") using a block holder (AFH-15, Avantes, Boulder, CO). This geometry was chosen to maximize specular reflectance, minimizing scattering within the bulk material (Willmouth, 1986). To quantify diffuse reflectance, we used an integrating sphere (AvaSphere-50-REFL; Avantes, Boulder, CO) equipped with a black gloss trap (AvaSphere-GT50, Avantes, Boulder, CO) to exclude specular reflectance. To quantify overall reflectance in a manner consistent with much of the previous avian color literature (Montgomerie, 2006), we collected spectral data at coincident normal (0° incident light/0° measurement) incidence using a bifurcated micron fiber optic probe held by a probe holder (RPH-1, Avantes) with matte black interior that excluded ambient light (hereafter, "coincident normal measurements"). For all three techniques, we took three measurements from each sample using AvaSoft software v.7.2, with the probe holder completely removed and placed at a different point on the feather

Fig. 2. Reflectance measurements from silver Anhinga feathers and white and gray feathers from other species. A–C: Reflectance spectra for (a) coincident normal (0° incident light/0° measurement), (b) specular (75° incident light/75° measurement), and (c) diffuse reflectance. Dashed, gray and blue lines are curves for white, gray and Anhinga feathers, respectively. D: Boxplots comparing brightness (mean reflectance across all wavelengths) between these feather types and for these reflectance types. White and gray boxes are data for white and gray feathers and blue "A"s with circles are data for Anhinga feathers. Small circles indicate outliers.

TABLE 1. Mean values (in % relative to a diffuse white standard) of feathers from different bird species for normal (R_N: 0°/0° incidence/measurement), specular (R_S: 75°/75°) and diffuse (R_D: multiple angles) reflectance. The ratio of specular to diffuse reflectance is a measurement of gloss

Species	Color	R_N (%)	R_S (%)	R_D (%)	R_S/R_D
Anhinga (*Anhinga anhinga*)	Silver	30.3	87.6	17.5	5.0
Glaucous gull (*Larus hyperboreus*)	White	64.6	94.4	38.6	2.4
Whistling swan (*Cygnus columbianus*)	White	46.3	101.8	36.3	2.8
Rock ptarmigan (*Lagopus muta*)	White	52.5	98.8	41.0	2.4
Caspian tern (*Hydroprogne caspia*)	White	68.9	111.4	48.7	2.3
European magpie (*Pica pica*)	White	57.1	114.5	41.3	2.8
Pine grosbeak (*Pinicola enucleator*)	Grey	15.7	24.0	6.1	3.2
Great blue heron (*Ardea herodias*)	Grey	11.3	20.9	6.5	4.3
House sparrow (*Passer domesticus*)	Grey	17.2	39.6	9.8	4.0
Grey Catbird (*Dumetella carolinensis*)	Grey	9.8	26.2	4.6	5.2
Tufted titmouse (*Baeolophus bicolor*)	Grey	9.5	45.3	11.5	3.9

surface before each measurement. For specular measurements, both barbule twisting in relation to the feather plane and the insertion angle of barbs and barbules can result in an angle-dependent variation in brightness if measurements are not taken perpendicular to the barbule reflectance plane (Osorio and Ham, 2002; Meadows et al., 2011). This means that, if the feather is held in a horizontal plane (i.e., has a tilt angle of 0°), the azimuth angle of maximum reflectance may not necessarily be parallel to the feather proximo-distal axis (i.e., when the holding block is parallel to the feather rachis). Thus, for specular measurements, we also rotated the holding block in relation to the feather plane to ensure that readings were taken at the azimuth angle of maximum reflectance (Osorio and Ham, 2002).

Refractive Index Matching

To determine if the silver color has a nanostructural basis, we coated feathers with wintergreen (*Gaultheria procumbens*) oil, which has an estimated refractive index (n) of 1.54 (Juliani et al., 1972), close to that of keratin (n = 1.56; Brink and van der Berg, 2004). Structural colors occur via interference of light scattering at interfaces between materials of different refractive indices, and by adding oil we effectively eliminated any variation in refractive index (Mason, 1923). Thus, we predicted that silver color would be lost after application of oil.

Microscopy and Optical Modelling

To characterize the microstructure and nanostructure responsible for producing silver color in these feathers, we used light microscopy and scanning and transmission electron microscopy (SEM and TEM, respectively). For SEM, we mounted feathers on stubs with carbon tape, sputter-coated them with silver and viewed them on a JEOL SEM. For light microscopy and TEM, we prepared samples following (Shawkey et al., 2003). Briefly, we cut barbs from the silver region of feathers, washed them in a solution of 0.1% Tween and 0.25 M NaOH, and fixed them in a 2:3 (v/v) solution of formic acid and ethanol. Next, we dehydrated the samples in 100% ethanol (twice for 20 min each time) and infiltrated them in 15, 50, 70, and 100% Epon (24 h each time). After curing the blocks at 60°C for 16 h in an oven, we trimmed them with a Leica S6 EM-Trim 2 (Leica Microsystems GmbH, Wetzlar, Germany) and cut 100-nm thin sections using a Leica UC-6 ultramicrotome (Leica Microsystems GmbH, Wetzlar, Germany). We stained these sections with uranyl acetate and lead citrate and viewed them on a Tecnai TEM (FEI, Hillsboro, OR, USA) at an operating voltage of 120 kV. For light microscopy, we cut 1–3 μm thick sections, transferred them with a loop to glass slides and viewed them on a Leica optical microscope.

Using these techniques, we identified two putative nanostructures in silver feathers (see results below), and used standard methods to identify how they may contribute to silver color production. For the array of keratin and melanin, we used ImageJ (available for download at http://rsb.info.nih.gov/nih-image/index.html) to measure the thickness of the keratin cortex and the thickness of the underlying layer of melanosomes at 10 evenly spaced locations along the dorsal surface of five separate barbules from two different barbs. We then used the mean of these values in standard transfer matrix thin-film optical models (Jellison, 1993) implemented in the statistical program R (R Core Development Team, 2007) using the *slmodels* function (Supplemental Material in Maia et al., 2009). We used previously published, empirically estimated refractive indices of air (n = 1.00), keratin (n = 1.56) and melanin (n = 2.00; Brink and van der Berg, 2004; Land, 1972), estimated lower limit extinction coefficients for keratin (k = 0.03) and eumelanin (k = 0.6; Brink and van der Berg, 2004; Land, 1972) as well as angles of incidence and reflectance matching those of our measured spectra in all of our calculations. We created a set of thin-film reflectance models, using all possible two- and three-beam combinations for the upper surface of the barbule. These models have been outlined numerous times (Doucet et al., 2006; Maia et al., 2009; Maia et al., 2010; Shawkey et al., 2006b). Model 1 included all three interfaces of materials of different refractive indices (air/keratin, keratin/melanin, melanin/keratin) and the thicknesses of the keratin and air layers. Model 2 included only the outer two interfaces (air/keratin, keratin/melanin) and the thickness of the keratin layer. Model 3 included only the air/keratin and melanin/keratin interfaces, and the thickness of the melanin layer. Model 4 included only the inner two interfaces (keratin/melanin, melanin/keratin) and the thickness of the melanin layer. We visually compared the spectra produced by these models to measured reflectance spectra from the feathers to determine which, if any, was most accurate.

For the amorphous spongy material, we analyzed cross-sectional TEM images using the Fourier tool for biological nanooptics (Prum and Torres, 2003). This MATLAB-based program uses Fourier analysis to determine whether nanostructures are sufficiently organized at an appropriate scale to produce color by coherent light scattering alone. Subsequent radial analyzes incorporating the estimated refractive indices of keratin (RI = 1.56) and air (RI = 1.00) allow the user to obtain a predicted hue. For all analyzes, the largest available square portion of keratin and air (>500 pixels) uninterrupted by melanin granules, cell boundaries or keratin cortex was selected.

RESULTS

Spectrometry

At coincident normal incidence, reflectance curves and values of silver feathers were intermediate between those of grey and white feathers (Fig. 2a,d). They contained no discrete peaks and instead showed rapidly increasing reflectance at short wavelengths (~300–400 nm), followed by more

gradually increasing reflectance at longer wavelengths. At specular incidence, curves of silver feathers were flat, similar to grey feathers, but with high reflectance (~80%), comparable to those of white feathers (Fig. 2b,d). Diffuse reflectance curves of silver feathers were again intermediate between those of white and grey feathers, but values were closer to those of grey feathers (Fig. 2c,d).

Refractive Index Matching

Coating silver feathers with an oil of refractive index close to that of keratin caused the color to immediately become black (Fig. 3), indicating that it is produced by light scattering (Mason, 1923).

Microscopy and Optical Modeling

Distal barbules are 2.5 times longer than proximal barbules, with highly elongated tips (pennula; Fig. 4). They are flattened, and show a gradient of melanization, starting at high concentration at the base and decreasing towards the pennulum (Figs. 4 and 5). In contrast, proximal barbules are completely melanized and show round pennula (Figs. 4 and 5). Distal barbules tightly interlock with the underlying adjacent row of black proximal barbules and extend covering the neighbor barb. On the feather's obverse ("dorsal") plane, the white portions of distal barbules are exposed, covering other melanized structures almost entirely. This overlapping results in a pattern of alternating wide white and thin dark bands (Figs. 3 and 4). Feathers are entirely black on their reverse ("ventral") plane (Fig. 3). Black and white portions of distal barbules can be seen either together or separately in cross-sections (Fig. 5b,c). When found together, black and white portions appear to be separated by cell boundaries, suggesting that they originate from separate cells (Fig. 5c).

Proximal sections of barbules had keratin cortexes with a mean thickness of 139.8 ± 7.5 nm, and weakly organized melanin layers (Fig. 6a). Similar quasi-ordered thin films have recently been shown to produce weakly chromatic glossy black color (Maia et al., 2010). The spectrum predicted by thin-film optical models 1and 4 had hue values (wavelength of peak reflectance) within 20 nm of that for the black portion of the feather surrounding the silver portion (Fig. 6b), suggesting that this nanostructure is capable of producing the observed glossy black color through interference. Model 1 is more likely to be accurate because model 4 predicts an additional peak in the UV (350 nm) that is not observed in the measured spectrum. The lack of fit between the tail ends of the modeled and measured spectra is likely due to the spectral noise produced by the weakly organized melanosome layer found in glossy barbules (see Supplemental Material in Maia et al., 2010).

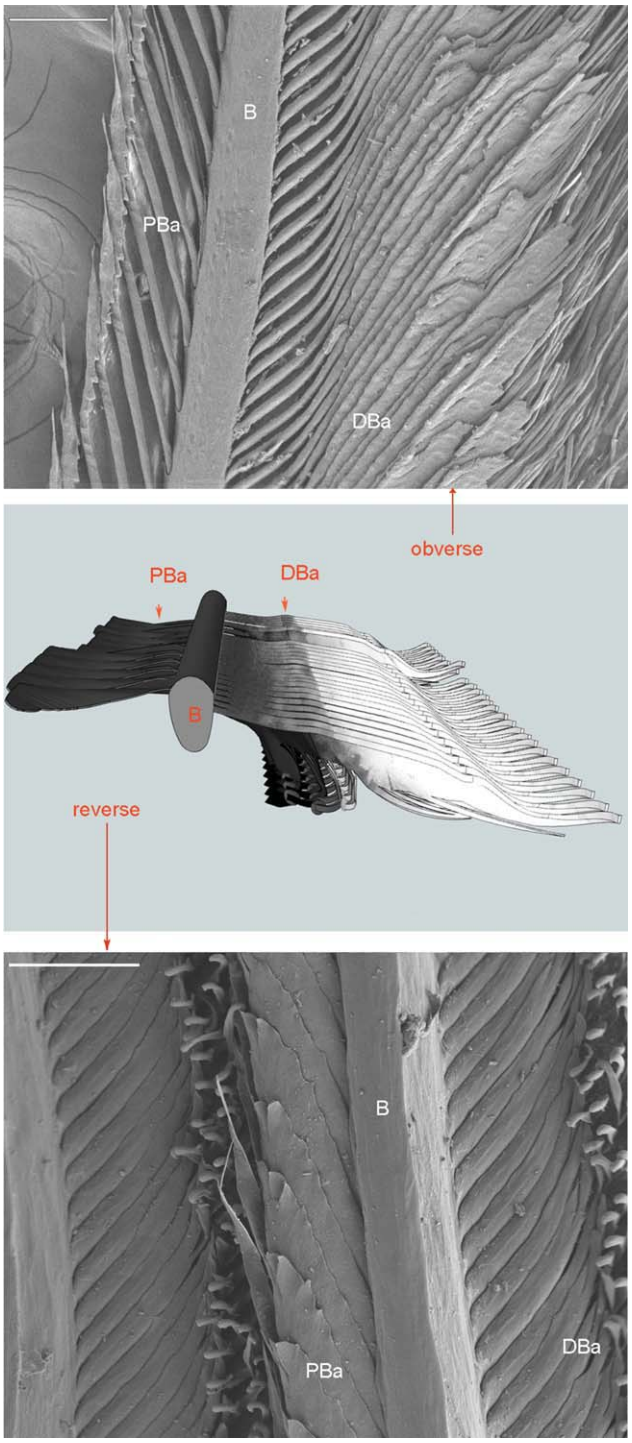

Fig. 4. Macrostructure of silver Anhinga feathers. Center: Cartoon of cross-section of a barb (B) showing the differentiation between the distal barbules (DBa) and the proximal barbules (PBa). Top: SEM of obverse side of feather, shows flattened and elongated white distal barbules and black proximal barbules (left). Bottom: Reverse side of feather, showing uniformly black distal and proximal barbules.

Distal sections of barbules in the silver portions of feathers contained an amorphous matrix of keratin and air (Fig. 7A). Fourier power spectra of

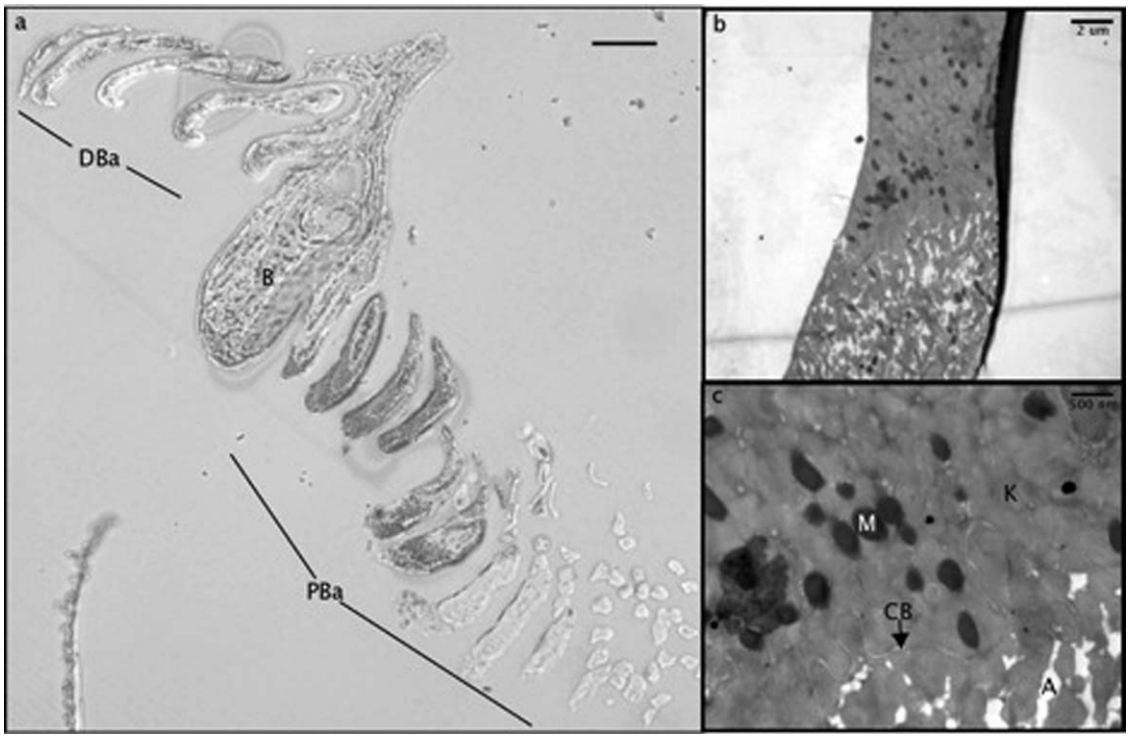

Fig. 5. Microstructure and nanostructure of silver Anhinga feathers. A: Light microscope image of a cross-section of barbs and barbules of a silver Anhinga scapular feather. Highlighted are the central barb (B), distal barbules (DBa) and proximal barbules (PBa). Dark spots are melanosomes. Note the melanized barb and proximal barbules, and the gradient of melanization in the proximal barbules. B: Transmission electron microscope image of a proximal barbule showing structured white (bottom) and unstructured (top) portions. The matrix of keratin (gray material) and air (white material) in the bottom portion likely produces white reflectance. C: Closeup of the central portion of the barbule in (B) showing cell boundaries between structured and unstructured portions, suggesting that they originate from separate cells. M = melanosomes, K = keratin, A = air, and CB = cell boundaries.

TEM cross-sections of this structure showed low power and an ovoid arrangement in Fourier space (Fig. 7B), suggesting weak order. Predicted spectra from these Fourier analyzes showed gradually increasing reflectance at longer wavelengths and no distinct peaks (Fig. 7C), similar to those from

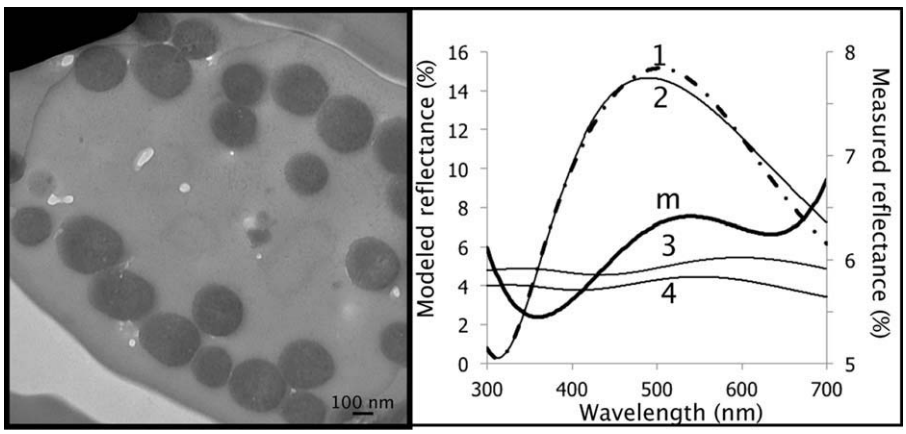

Fig. 6. Nanostructure likely producing glossy black color in silver Anhinga feathers. A: Transmission electron microscope image of a barbule from a silver Anhinga feather showing a quasi-ordered array of melanosomes (dark circles) bounding a thin outer keratin cortex. B: Measured (from the black outer portion of an Anhinga scapular feather; solid line) and predicted (dashed line) reflectance from the black portion of a silver Anhinga feather at coincident normal incidence. Predicted measurements are based on four thin film models (numbered 1–4). Model 1 included all three interfaces of materials of different refractive indices (air/keratin, keratin/melanin, melanin/keratin) and the thicknesses of the keratin and air layers. Model 2 included only the outer two interfaces (air/keratin, keratin/melanin) and the thickness of the keratin layer. Model 3 included only the air/keratin and melanin/keratin interfaces, and the thickness of the melanin layer. Model 4 included only the inner two interfaces (keratin/melanin, melanin/keratin) and the thickness of the melanin layer. *m* = measured reflectance spectrum.

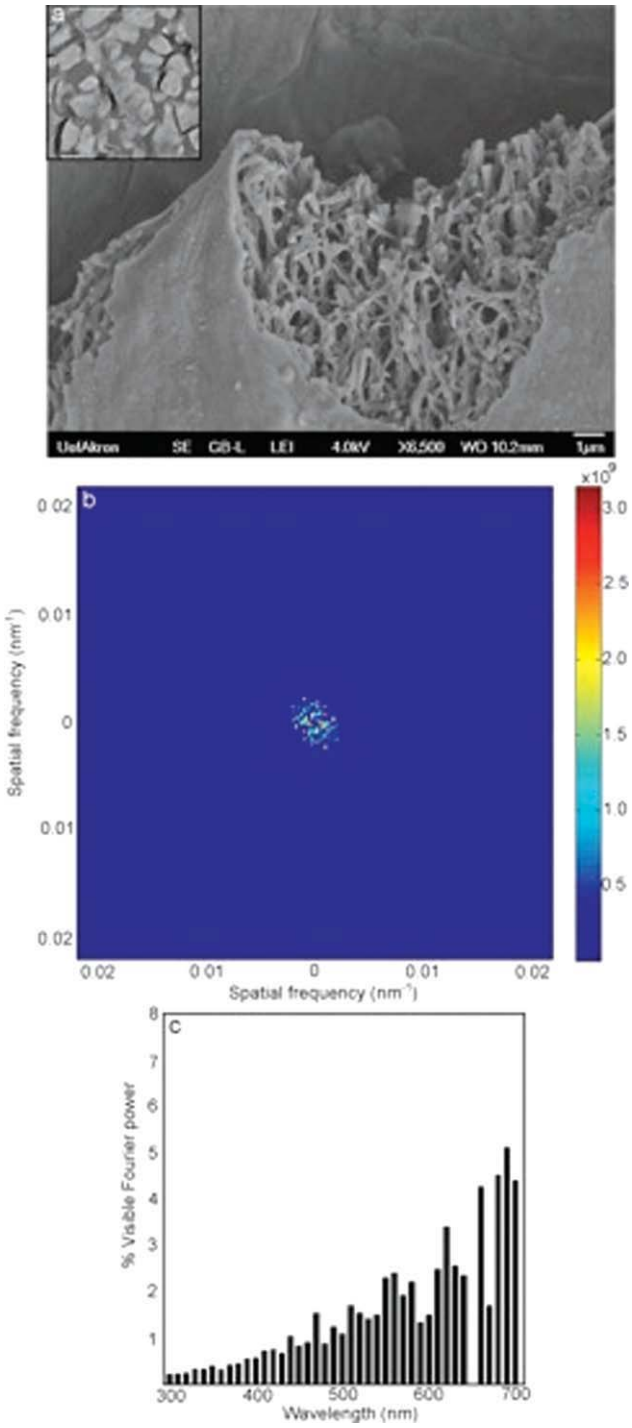

Fig. 7. Optical analysis of nanostructure likely producing white reflectance in silver Anhinga feathers. A: Scanning electron microscope image showing a barbule with the outer layer partially removed to reveal the amorphous matrix of keratin and air. Inset: Transmission electron microscope image of this matrix. B: Fourier power spectrum of TEM image showing weak order. C: Predicted reflectance based on Fourier analysis. [Color figure can be viewed in the online issue, which is available at wileyonlinelibrary.com.]

other unordered systems (Shawkey and Hill, 2006). This nanostructure thus appears to produce white color through incoherent, or weakly coherent scattering.

DISCUSSION

Our data suggest that the distinctive silvery color of Anhinga feathers is primarily a result of high gloss that distinguishes it from all white and most gray feathers examined. However, a gray feather (from a Grey Catbird) with comparable gloss but lower diffuse and specular reflectance did not have a silvery appearance (see Fig. 2d). This suggests that high absolute values of these two reflectance components, as well as high gloss, are necessary for silver color. Light and electron microscopy revealed that feathers are not uniformly silver but rather have barbules with discrete white and black components that are produced by a hierarchy of separate nanostructures. The white component appears to be a disorganized amorphous matrix of keratin and air, while the black component is a quasi-ordered thin-film. This mechanism is completely distinct from those producing metallic colors in invertebrates (Seago et al., 2008) or fish (Levy-Lior et al., 2010) and, as far as we are aware, this is the first time that multiple nanostructural arrangements have been found in barbules.

The amorphous matrix appears to be a rare but divergently distributed mechanism of white color production. Generally, white colors in birds and arthropods are produced by incoherent light scattering at the interface of keratin and air at the integumental surface or in central air vacuoles in their interior (Prum, 2006). For example, barbs of white chicken feathers consist of a single thick layer of unstructured keratin over a large central air vacuole (Shawkey and Hill, 2006). Modifications that increase the number of scattering elements (i.e., the number of interfaces of materials with different refractive indices) may increase the intensity of this white color. In arthropods, densely packed beads within scales of Pierid butterflies dramatically increase their white reflectance (Stavenga et al., 2004) and bright white color in a *Cyphochilus* beetle (Vukusic et al., 2007) is caused by incoherent scattering from a matrix of unorganized air spaces within a chitin matrix. In the rock ptarmigan, an amorphous matrix causes feather color to be similar to, and hence camouflaged in, snow (Dyck, 1979). The white nanostructure described here is similar to those of both the ptarmigan and the beetle, suggesting convergent evolution in distantly related organisms that use different primary structural materials (keratin vs. chitin). It also resembles relatively more ordered amorphous nanostructures (spongy layers) that produce noniridescent blues and violets via coher-

ent scattering, which are relatively common in feather barbs (Prum, 2006) but have not been observed in arthropods. It has recently been hypothesized that avian spongy layers ontogenetically develop through processes of self-assembly through phase separation (specifically, spinodal decomposition and nucleation and growth) and that a change in one or a few parameters (keratin concentration, speed of polymerization, etc.) may produce quasi-ordered matrices and thus coherent light scattering (Dufresne et al., 2009; Prum et al., 2009). Why similar effects may only produce unorganized matrices in feather barbules is unknown but should be considered in the future.

This white nanostructure is morphologically intermediate between unstructured white barbs/barbules and quasi-ordered spongy layers. Similarly, the glossy black structure is intermediate between those of matte black and iridescent barbules (Maia et al., 2010). These latter nanostructures produce high specular reflectance and thus should contribute to the high specular reflectance of Anhinga feathers. Indeed, the outer black portion of the Anhinga feather had the low overall reflectance ($<$7%) and weak reflectance peak ($\sim$1.5% difference between minimum and maximum reflectance) characteristic of highly specular glossy black feathers (Maia et al., 2010).

White and black barbule portions appear to have their developmental origins in separate cells. Cellular membranes were seen in barbule cross-sections spanning the black and white regions of the barbules, suggesting that these cells connect forming several rows (i.e., on the obverse–reverse plane) in barbule ridges. Barbules are typically composed of one single row of cells (Alibardi, 2006), so having multiple rows of cells appears to be another modification of typical barbule structure in these feathers. This complexity is surprising because these structures have apparently convergently evolved multiple times in distantly related lineages (Galván et al., 2009). However, overall the modifications do not appear to be major reorganizations. The deposition of melanin in a proximo-distal gradient fits the proposed reaction–diffusion model of pigment deposition in developing feathers (Prum and Williamson, 2002), and thus does not require any new innovations. While the ontogeny of the black and white nanostructures is poorly understood, we hypothesize that they develop through processes of self-assembly through phase separation fundamentally similar to those in spongy layers (Dufresne et al., 2009; Prum et al., 2009). Thus, Anhingas may exploit processes commonly used in feather development to generate entirely novel structures.

The selection pressures leading to this novel combination of structures are likely numerous. Anhinga contour feathers are known to be less hydrophobic than feathers of other species, decreasing buoyancy and allowing for greater maneuverability underwater (Owre, 1967). In contour feathers, this is largely caused by the lack of hooklets holding barbules together. The highly modified, flattened barbules of silver scapular and covert feathers may also decrease hydrophobicity by increasing available surface area for water absorption (i.e., by increasing barbule fraction area in Cassie–Baxter wetting theory, see Bormashenko et al., 2007; Eliason and Shawkey, in press). This modification may allow, or be a result of, the amorphous white matrix. Because dry feathers trap air, they play an effective role in bird thermoregulation (Stettenheim, 2000). Thus, decreased hydrophobicity would impair thermoregulation and would necessitate drying of feathers in the sun. Black feathers should dry fastest due to their ability to absorb light, although empirical support for this idea in the literature is lacking. This may help explain why the feathers most critical to flight (primaries and secondaries) are black while presumably slower drying silver feathers are restricted to less essential feathers. Anhingas are sexually dichromatic (Frederick and Siegel-Causey, 2000), but not in their silver coloration, and males retain silver feathers in their nonbreeding plumage. Both of these facts argue against a strong role for classical sexual selection. However, cryptic UV dichromatism in silver feathers (Bennett et al., 1994) or mutual mate choice can not be ruled out at this point. Finally, this method of producing silver coloration may also be useful for novel paints or other coatings. Future research on silver feathers will span multiple disciplines (development, optics, evolution) and thus has the potential to be truly integrative.

ACKNOWLEDGMENTS

We thank C.M. Eliason and two anonymous referees for helpful comments.

LITERATURE CITED

Alibardi L. 2006. Cells of embryonic and regenerating germinal layers within barb ridges: Implication for the development, evolution and diversification of feathers. J Submicrosc Cytol Pathol 38:51–76.

Bennett ATD, Cuthill IC, Norris KJ. 1994. Sexual selection and the mismeasure of color. Am Nat 144:848–860.

Bormashenko Y, Stein T, Whyman G, Bormashenko E. 2007. Why do pigeon feathers repel water? Hydrophobicity of pennae, Cassie–Baxter wetting hypothesis and Cassie–Wenzel capillarity-induced wetting transition. J Colloid Interface Sci 311:212–216.

Brink DJ, van der Berg NG. 2004. Structural colours from feathers of the bird *Bostrychia hagedash*. J Phys D: Appl Phys 37:813–818.

Chandler A. 1916. A study of the structure of feathers: With reference to their taxonomic significance. University of California Publications in Zoology 13:243–447.

D'Alba L, Saranathan V, Clarke JA, Vinther JA, Prum RO, Shawkey MD. 2011. Colour-producing β-keratin nanofibres in blue

penguin (*Eudyptula minor*) feathers. Biol Lett 2011 Feb 9; [Epub ahead of print (doi:10.1098/rsbl.2010.1163)].
Doucet SM, Shawkey MD, Hill GE, Montgomerie R. 2006. Iridescent structural plumage coloration in satin bowerbirds: Structure, mechanisms and individual variation. J Exp Biol 209:380–390.
Dufresne ER, Noh H, Saranathan V, Mochrie SGJ, Cao H, Prum RO. 2009. Self-assembly of amorphous biophotonic nanostructures by phase separation. Soft Matter 5:1792–1795.
Dyck J. 1979. Winter plumage of the rock ptarmigan: Structure of the air-filled barbules and function of the white colour. Dansk orn Foren Tidsskr 73:41–58.
Eliason CM, Shawkey MD. 2011. Decreased hydrophobicity of iridescent feathers: A potential cost of shiny plumage. J Exp Biol 214:2157–2163.
Fox DL. 1976. Animal Biochromes and Structural Colours. Berkeley, CA: University of California Press.
Frederick PC, Siegel-Causey D. 2000. Anhinga (*Anhinga anhinga*). In: Poole A, editor. The Birds of North America Online. Ithaca: Cornell Lab of Ornithology.
Galván I, Negro JJ, Bortolotti GR, Margalida A. 2009. On silver wings: A fragile structural mechanism increases plumage conspicuousness. J Avian Biol 40:475–480.
Hill GE, McGraw KJ, editors. 2006. Bird Coloration Vol. I: Mechanisms and Measurements. Boston: Havard University Press.
Jellison G Jr. 1993. Data analysis for spectroscopic ellipsometry. Thin Solid Films 234:416–422.
Juliani R, Moharram H, Wang M, Simon J. 1972. Chemical diversity of Nepales essentail oils. New Use Agriculture and Natural Plant Products Program. Cook College: Rutgers University.
Land MF. 1972. The physics and biology of animal reflectors. Prog Biophys Mol Bio 24:77–106.
Levy-Lior A, Shimoni E, Schwartz O, Gavish-Regev E, Oron D, Oxford G, Weiner S, Addadi L. 2010. Guanine-based biogenic photonic-crystal arrays in fish and spiders. Adv Funct Mater 20:320–329.
Maia R, Caetano JVO, Bao SN, Macedo RH. 2009. Iridescent structural colour production in male blue–black grassquit feather barbules: The role of keratin and melanin. J R Soc Interface 6:S203–211.
Maia R, D'Alba L, Shawkey MD. 2010. What makes a feather shine? A nanostructural basis for glossy black colors in birds. Proc R Soc Lond B published online 2010.
Mason CW. 1923. Structural colors in feathers. J Phys Chem 27:201–251.
Meadows MG, Morehouse NI, Rutowski RL, Douglas JM, McGraw KJ. 2011. Quantifying iridescent coloration in animals: A method for improving repeatability. Behav Ecol Sociobiol; DOI: 10.1007/s00265-010-1135–5.
Montgomerie R. 2006. Analyzing colors. In: Hill GE, McGraw KJ, editors. Bird Coloration. Cambridge, MA: Harvard University Press. pp90–147.
Nassau K. 1983. The Physics and Chemistry of Color: The Fifteen Causes of Color. New York: Wiley and Sons.
Nickerson D. 1957. A new cotton lustermeter for yarns and fibers. Text Res J 27:111–123.
Osorio D, Ham A. 2002. Spectral reflectance and directional properties of structural coloration in bird plumage. J Exp Biol 205:2017–2027.
Owre OT. 1967. Adaptations for locomotion and feeding in the Anhinga and the double-crested cormorant. Ornithol Monogr 6:1–138.
Prum RO. 2006. Anatomy, physics and evolution of avian structural colors. In: Hill GE, McGraw KJ, editors. Bird Coloration: Mechanisms, Vol. I: Mechanisms and Measurements. Boston: Harvard University Press.
Prum RO, Dufresne ER, Quinn T, Waters K. 2009. Development of colour-producing beta-keratin nanostructures in avian feather barbs. J R Soc Interface 6:S253–S265.
Prum RO, Torres RH. 2003. A Fourier tool for the analysis of coherent light scattering by bio-optical nanostructures. Integr Comp Biol 43:591–602.
Prum RO, Williamson S. 2002. Reaction-diffusion models of within-feather pigmentation patterning. Proc R Soc Lond B 269:781–792.
R Core Development Team. 2007. R: A Language for Data Analysis and Graphics. Vienna, Austria: R Foundation for Statistical Computing.
Rasmussen P, Dyck J. 2000. Silkiness in brown mink pelts characterized with optical methods. J Anim Sci 78:1697–1709.
Seago A, Brady P, Vigneron JP, Schultz T. 2008. Gold bugs and beyond: A review of iridescence and structural colour mechanisms in beetles (Coleoptera). J R Soc Interface 6:S165–S184.
Shawkey MD, Estes AM, Siefferman LM, Hill GE. 2003. Nanostructure predicts intraspecific variation in ultraviolet-blue plumage colours. Proc R Soc Lond B 270:1455–1460.
Shawkey MD, Balenger SL, Hill GE, Johnson LS, Keyser AJ, Hill GE. 2006a. Mechanisms of evolutionary change in structural plumage coloration among bluebirds (*Sialia* spp.). J R Soc Interface 3:527–532.
Shawkey MD, Hauber ME, Estep LK, Hill GE. 2006b. Evolutionary transitions and structural mechanisms of avian plumage coloration in grackles and allies (Icteridae). J R Soc Interface 3:777–783.
Shawkey MD, Hill GE. 2006. Significance of a basal melanin layer to production of non-iridescent structural plumage colour: Evidence from an amelanotic Steller's jay (*Cyanocitta stelleri*). J Exp Biol 209:1245–1250.
Shawkey MD, Morehouse NI, Vukusic PR. 2009. A protean palette: Color materials and mixing in birds and butterflies. J R Soc Interface 6:S221–S231.
Stavenga DG, Stowe S, Siebke K, Zeil J, Arikawa K. 2004. Butterfly wing colours: Scale beads make white pierid wings brighter. Proc R Soc Lond B 271:1577–1584.
Stettenheim PR. 2000. The integumentary morphology of modern birds—an overview. Am Zool 40:461–477.
Toomey MB, Butler MW, Meadows MG, Taylor LA, Fokidis HB, McGraw KJ. 2010. A novel method for quantifying the glossiness of animals. Behav Ecol Sociobiol 64:1047–1055.
Vukusic P, Hallam B, Noyes J. 2007. Brilliant whiteness in ultrathin beetle scales. Science 315:348.
Willmouth FM. 1986. Transparency, translucency and gloss. In: Meeten GH, editor. Optical Properties of Polymers. London: Elsevier Applied Science Publishers Ltd. pp265–334.